High Temperatures - High Pressures, 1975, volume 7, pages 331-340

Card made

Press calibration at elevated temperatures

D L Decker, J D Jorgensen¶, R W Young
Department of Physics and Astronomy, Brigham Young University, Provo, Utah 84602, USA

Received 22 July 1975

Abstract. The pressure increase upon heating an internal liquid cell in a pyrophyllite pressure chamber within a multi-anvil press was determined by simultaneously measuring the phase diagrams of bismuth and mercury to 55 kbar and comparing them with the established phase diagrams. The shapes of the differential thermal analysis signals are used to establish equilibrium values of the phase lines. Phase diagrams for thallium, tin, indium, and lead are reported.

1 Introduction

For the past several years we have struggled with the problem of how to measure pressure accurately in an internally heated pressure chamber within a multi-anvil pressure cell. Some of these problems have been reviewed earlier by Decker *et al.* (1972). Even if one has a means of calibrating the pressure versus load using fixed point phase transitions, one does not know the pressure at higher temperatures because of thermal expansion of the pressure cell on heating. Experiments which attempt to measure the pressure dependence of melting curves and diffusion measurements at high pressure, to mention two, would be greatly improved by a means of determining the pressure at elevated temperatures. Earlier attempts by Decker and Vanfleet (1965), Mitra *et al.* (1967), and Millet and Decker (1969) assumed a Simon's equation for the melting curve; the pressure calibration was adjusted to cause the melting curve to take this form. Various arguments were given to justify a certain pressure and temperature dependence of the pressure correction. A second approach by Young (1969) involved measuring the lattice parameter of NaCl at high pressure and elevated temperatures and obtaining the pressure from a theoretical equation of state by Decker (1965). This method did show pressure changes with heating, but only for a pressure cell of the material and construction of that used for x-ray work. It is not clear how to interpret these results for an internally heated liquid cell for example. A third attempt by Candland *et al.* (1972) consisted of measuring the resistance of a Manganin wire over a range of pressure and temperature in a liquid medium within a large-volume pressure cell. The results were interpreted by extrapolating the Manganin room-temperature pressure calibration to higher temperatures with the use of the measurements of Wang (1967) to 250°C and 4 kbar as a guide to the extrapolation. The major drawback to this approach is the large extrapolation which makes the results rather uncertain.

In the present experiment, we determine the pressures from a knowledge of certain fairly well studied phase diagrams. One can use either two materials and measure transitions between their phases at elevated pressures, or a single substance, such as bismuth, with several phases. The philosophy is very simple. If one knows $P(T)$ along two lines in P, T space, then maintaining a constant load one raises the temperature crossing these two known lines at T_1 and T_2 and from the known relations one has also P_1 and P_2 so a pressure versus temperature increase is measured of value $(P_2-P_1)/(T_2-T_1)$.

¶ Present address: Argonne National Laboratory, Argonne, Illinois, USA.

2 Experimental procedure

We simultaneously measured the phase diagrams of mercury with bismuth, thallium, tin, and lead, as well as the phase diagram of bismuth alone. Two types of samples were used, both of them in a hydrostatic liquid environment in which the phase changes are sharp and distinct. In the first case about 100 mg of bismuth was placed in a boron nitride cup (4·7 mm diameter and 4 mm deep) and a thermocouple was embedded in the bismuth while molten. This was placed in a thin-wall Inconel can, 6·3 mm inside diameter and 2·4 cm long, which was filled with petroleum ether and capped at each end with polyethylene plugs. Electrical current was sent through the can causing the temperature to rise slowly (between 0·1 and 1 K s^{-1}) while observing the thermal arrest as the bismuth underwent phase transitions. This was repeated at many constant loads. The pressure at each phase change was determined from the measured temperature on the assumption that the phase diagram of bismuth is known. This last assumption is likely to be quite valid for the measurements of Tikhomirova *et al.* (1966) in liquid systems below about 30 kbar. The temperatures were determined from the e.m.f. of the Chromel–Alumel thermocouple and corrected for the effects of pressure by averaging the measurements of Getting and Kennedy (1970) and Hanneman *et al.* (1971). This correction to the e.m.f. due to pressure on the thermocouple junction is less than 1·2 K at any point in this experiment and is small enough not to contribute more than a 0·1 kbar error at any pressure. The thermocouples were calibrated at atmospheric pressure against the melting points of indium, tin, lead, and zinc. To get the pressure increase with heating we took the pressure at room temperature, 26°C, from a calibration against load—determined from a fixed-point calibration with the phase changes Hg L–I, Bi I–II, and Tl I–II taken as a 12·6, 25·6, and 38 kbar respectively—all measured on increasing pressure only. From this pressure at room temperature and that at the

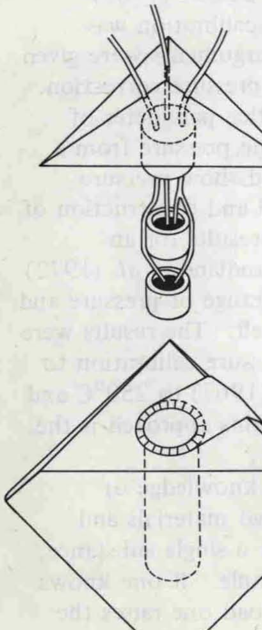

Figure 1. A diagram of the pressure cell. A pyrophyllite cube, 2·45 cm along an edge, contains a liquid-filled chamber into which the specimens are inserted. The specimens are in polyethylene cups. The wires entering through the edges of the cube are thermocouple wires.

bismuth phase changes at the same load, we determined the pressure increase on heating at a constant press load.

In the second type experiment differential thermocouple techniques were used. Two samples (one of which was mercury in each case) were placed in polyethylene buckets as shown in figure 1 and a thermocouple junction was affixed to each. The thermocouple leads were arranged such that we could measure the e.m.f. of the junction in mercury or in the other junction simultaneously with the difference between the two junctions. We also used as a reference an ice bath junction outside the pressure chamber. The pressure was increased slowly until the mercury L–I transition was observed from the latent heat release causing the temperature of mercury to rise above that of the other sample. The temperature was then slowly increased at constant load, and the thermocouple difference signal referred to the temperature of mercury was observed and the phase changes were noted. We then assumed that the melting curve of mercury proposed by Bogdanov *et al.* (1971) was accurate, at least below about 40 kbar, and that the phase changes of bismuth below 30 kbar were known. From these we determined the value of $\Delta P/\Delta T$ between the mercury and bismuth phases.

3 Results

Figure 2 shows the DTA signal as the mercury and bismuth passed through phase changes at room temperature upon increasing the press load. The Hg L–I and Bi I–II transitions were used in determining the room-temperature pressure calibration.

The shapes of the differential signals at the phase transitions upon changing the temperature at fixed load are shown in figures 3–5. It is noted that the Hg I–L (melting transition) as shown in figure 3a is extremely sharp with a small amount of hysteresis (<2 K) on solidification. After this initial supercooling the temperature rises to the melting value so that the Hg I–L indication is repeatable to ±0·2 K. All the melting signals are similar to that of mercury, provided the samples are pure and do not alloy with the thermocouple or other contact materials. It was noted that the lead samples appeared to alloy with the thermocouple at temperatures above 550°C and that bismuth in a steel container alloyed with the steel above 350°C. This manifested itself as a rounding of the DTA signal and often some spreading of the signal. The solid–solid phase changes are more difficult to analyze. In general there is both supercooling and superheating beyond the equilibrium temperature. This is clear in the Hg I–II signal in figure 3b. In this case it is apparent that the Hg II–I signal is much nearer the equilibrium value than the Hg I–II signal. If the DTA signals are essentially alike on increasing and decreasing temperature one might assume the equilibrium value to be midway between these points. Unfortunately, some transitions show very large hysteresis, particularly at lower temperatures, thus making a precise determination of the equilibrium temperature impossible. The signals in figures 4 and 5 show various bismuth transitions near the triple points on the phase diagram. The thermal arrest signals are not vertical because they are plotted against the temperature measured with the thermocouple recording the temperature of mercury which was changing during the phase transition of bismuth. This is most clearly observed in the bismuth melting signal in figure 5.

In the first type of experiment, in which we measured the several bismuth phase changes and used the room-temperature pressure–load calibration, we determined a pressure increase with heating at constant load of $\Delta P/\Delta T = 0{\cdot}016$ kbar K^{-1} at pressures below 30 kbar. The phase diagram of bismuth above 30 kbar appears to be more inaccurate, for, if we take the phase lines reported by Klement *et al.* (1963b) and Haygarth *et al.* (1969) who used a piston cylinder apparatus, the value of $\Delta P/\Delta T$ suddenly jumps to $0{\cdot}022$ kbar K^{-1} above the IV–V–L triple point. We also find a

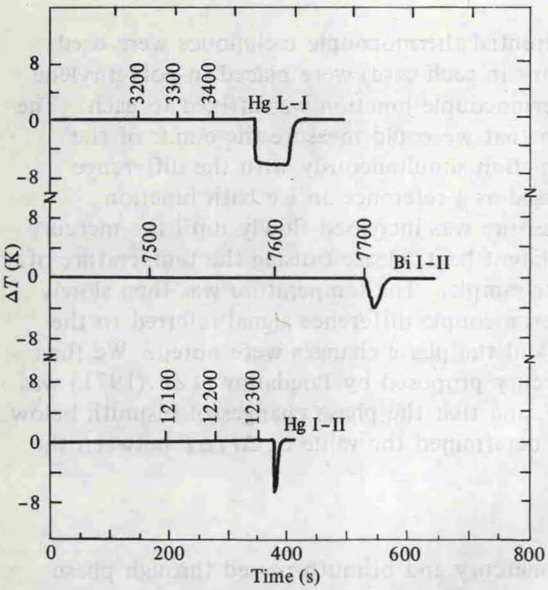

Figure 2. DTA signals upon passing through the Hg L–I, the Bi I–II, and the Hg I–II phase changes at room temperature on increasing the press load. The press load (lb in^{-2}) is indicated by the numbers along the recorder trace.

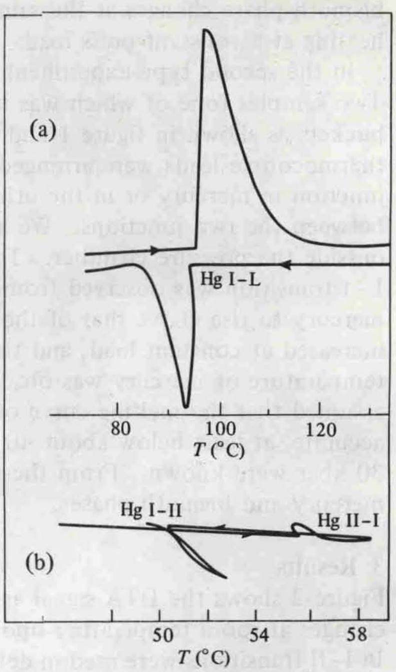

Figure 3. DTA signals at (a) the Hg I–L and (b) the Hg II–I phase transitions on increasing and decreasing the temperature near 47 kbar.

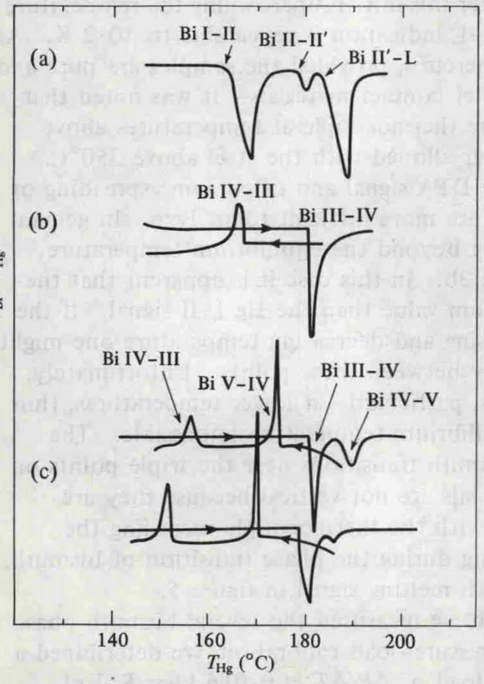

Figure 4. DTA signals at the phase changes of bismuth: (a) near 19 kbar, showing the presence of the II′ phase; (b) near 36 kbar—note the types of hysteresis in this transition; and (c) 50·9 and 51·3 kbar, just below the III–IV–V triple point.

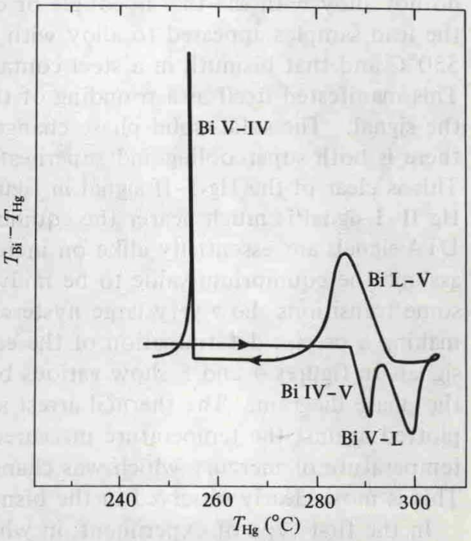

Figure 5. DTA signals near the Bi IV–V–L triple point. Note that the nature of the IV–V and V–IV transitions is the same as that shown in figure 4. The melting signal is not vertical because the temperature at the mercury junction is changing while the bismuth is going through the phase change.

different value for $\Delta P/\Delta T$ between room temperature and the Bi IV–V phase line than between room temperature and the Bi V–L melting point. At these pressures our pressure cell should be essentially a constant volume system and we could expect $(\partial P/\partial T)_V$ to be nearly constant, independent of pressure or temperature. Thus we assumed $\Delta P/\Delta T = 0{\cdot}016$ kbar K^{-1} over the entire temperature and pressure range of our measurements. This makes the data consistent but gives triple points at lower pressures than those reported by workers who used piston-cylinder devices with a solid pressure-transmitting medium. The triple points of bismuth are shown in table 1 and the phase diagram of bismuth is shown in figure 6. The slanted

Table 1. Triple points in the phase diagram of bismuth (°C/kbar).

Investigator	I–II′–L	I–II–II′	II–II′–L	II–IV–L	II–III–IV	IV–V–L	III–IV–V
Bridgman (1935)	183/17·0			185/22·0			
Butuzov and Ponyatovskii[a] (1956)	184/17·0			184/22·0			
Ponyatovskii[a] (1960)					174/22·2		
Klement *et al.*[b] (1963b)	191/16·7			191/23·6	180/24·0	296/38·0	174/52·6
Tikhomirova *et al.*[b] (1966)	192/16·9	182/17·6	191/19·9	191/21·4	182/21·9		
Haygarth *et al.*[b] (1969)							175/54·3
This work[c]	192/17·1	183/17·8	191/19·7	190/21·8	184/22·2	294/37·0	186/51·8

[a] Average of transitions upon increasing and decreasing the temperature.
[b] The values upon increasing temperature only.
[c] Equilibrium values.

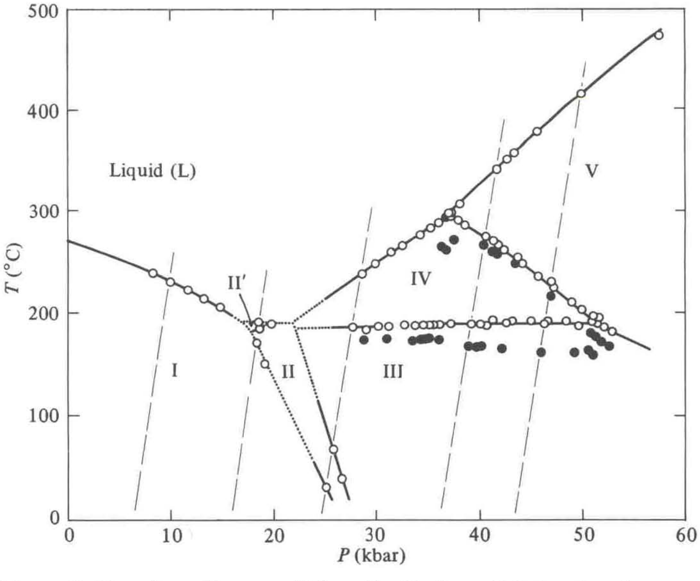

Figure 6. The phase diagram of bismuth. Each small dot and each open circle represent a separate measurement of the phase transitions upon increasing temperature. The solid circles are phase transitions on decreasing temperature. The lines represent equilibrium values for the transitions estimated by considering the shapes of the DTA signals at the transitions. The dashed lines indicate the pressure–temperature path at constant press load.

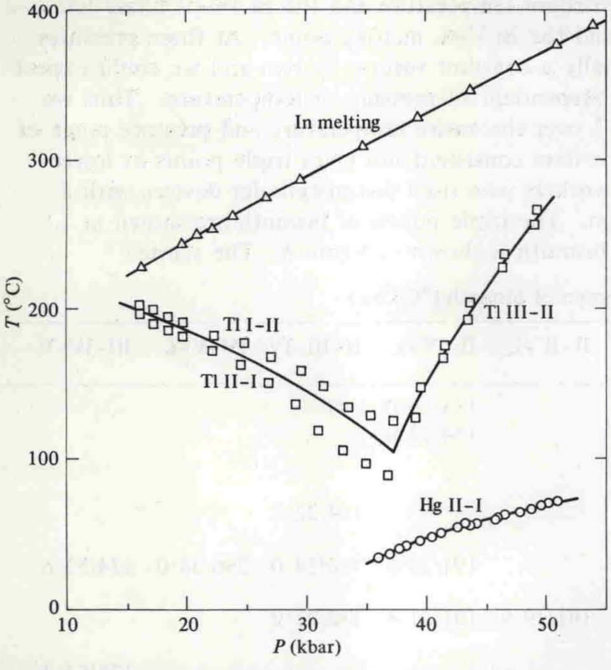

Figure 7. Equilibrium phase lines for indium, thallium, and mercury. The transitions at both increasing and decreasing temperatures are shown for thallium. The mercury points are taken from six separate measurements. This shows the repeatability of the measurements.

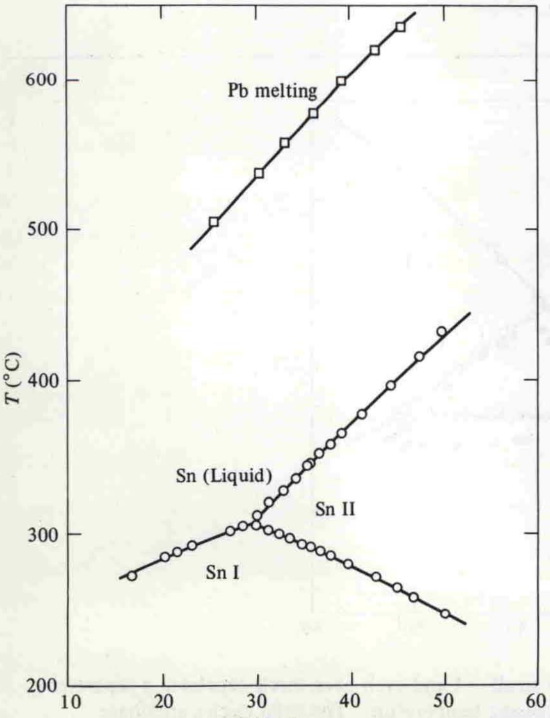

Figure 8. Equilibrium phase diagrams for lead and tin.

lines in this figure are the heating curves at constant load. It is to be noted that we clearly observed the II′ phase as reported by Tikhomirova *et al.* (1966). All the phase lines shown are for the transition as it first takes place upon increasing the temperature across the phase boundary.

In the second type of experiment, in which we compared the phase diagram of bismuth against the melting curve of mercury, we again obtained $\Delta P/\Delta T = 0\cdot016$ kbar K^{-1} below 30 kbar where the phase changes of these materials are accurately known. If we again assume the same value at higher pressures we reproduce the same phase diagram for bismuth as shown in figure 6. The Bi II′ phase was again observed and the Bi II–II′ transition signal is shown in figure 4a. The other transitions of bismuth shown in figures 4 and 5 are near various triple points. For these measurements we assumed the melting curve of mercury of Bogdanov *et al.* (1971) to be accurate to 30 kbar and used their extrapolation to 50 kbar.

Once we had a value for $\Delta P/\Delta T$, we measured the phase diagrams for lead, thallium, tin, indium, and mercury to check the consistency of our results. In figures 7 and 8 we show the phase diagrams for these materials. The Tl I–II phase line was not observed for it was so steep that no latent-heat signal appeared upon heating through this region.

4 Discussion and conclusions

Pressures calculated from the melting curve of mercury of Bogdanov *et al.* (1971) are estimated to be accurate to ±0·5% between 10 and 30 kbar, and in the extrapolation from 30 to 40 kbar accurate to ±1%. The only other measurements of the melting curve of mercury above 30 kbar are those of Klement *et al.* (1963a), which agree to within 0·1 kbar with those of Bogdanov *et al.* to 30 kbar, but are higher in pressure than the extrapolation of Bogdanov *et al.* by 1·5 kbar at 40 kbar and 6 kbar at 55 kbar. This discrepancy is considerably larger than the uncertainty estimated by these authors. The pressures estimated at Kennedy's laboratory at that time, however, were likely to be too high as was noted in the results for bismuth reported above. Thus the pressure at the melting curve of mercury is not as well known as we would desire for this work.

The only other measurement of the Hg II–I phase line is by Klement *et al.* (1963a), and their results are consistently 3 K below ours. Their measurements were, however, taken as the average of the signals upon increasing and decreasing the temperature through the phase lines. They observed 6 K hysteresis at 42 kbar. Our results are taken at the II–I phase change on increasing temperature. This choice was made because of the shape of the DTA signals which indicated this transition to be much nearer the equilibrium conditions for the transition. (Note the large supercooling effects observed for the II–I transition in figure 3b.) These measurements and those of Klement *et al.* are thus in extremely good agreement. If we had used their melting curve of mercury for our calibration rather than the extrapolation of Bogdanov *et al.*, we would have had a 5·6 kbar disagreement with the Hg II–I line of Klement *et al.* near 50 kbar. This is an indication of a discrepancy between the pressure measured by Klement *et al.* near room temperature and those measured at higher temperatures at these pressures, or of an error in our $\Delta P/\Delta T$. The latter would require a value of 7·2 kbar/100 K which is completely impossible when considering the rest of our data.

The melting curve of indium runs nearly parallel to the melting curve of mercury and is 170 K above it. The pressure correction due to heating above the mercury calibration would thus be 2·7 kbar all along the curve. The measured melting line is in good agreement with the one reported by Millet (1968) but is 1 kbar below that of Jayaraman *et al.* (1963) at 20 kbar and 6 kbar below their value at 50 kbar. Our results for indium, however, may be too high in temperature because the solidification signal always came at a higher temperature than the melting signal which showed a slight rounding. These effects indicate a possible alloying, so this curve could be as much as 10 K too high at the largest pressures.

The melting curve of lead is 2·5 kbar lower than the measurements of Akella *et al.* (1973) at 50 kbar and 1 kbar below theirs at 25 kbar. Our results are about 1 kbar above those of Millet (1968) in this same range. Again, as with indium, we found some rounding in the melting signal and a tendency for the solidification points to lie at higher temperatures than the melting points; thus our results may have an uncertainty as large as 2 kbar at the highest pressure point. If we used the melting curve of mercury due to Klement *et al.* (1963a), however, rather than the extrapolation of Bogdanov *et al.* (1971) for our pressure standard we would find our pressures to be 1·5 kbar above those of Akella *et al.* at the highest points. The parameter $\Delta P/\Delta T$ must be 1·6 ± 0·2 kbar/100 K for our liquid cell in order to get any reasonable agreement between our results and those of Akella, confirming our measurement of this parameter.

The phase diagram of thallium agrees well with that of Jayaraman *et al.* (1963) to the triple point, but their pressures are 2 kbar higher than ours at 50 kbar along with the III–I phase line. We chose the equilibrium values for the transitions as midway between the up and down transitions which showed considerable hysteresis, especially near the triple point. This choice is motivated by the symmetrical shape of the transitions shown in figure 9a. Our II–I phase line shows more curvature than that of Jayaraman *et al.* We measured $(\mathrm{d}T/\mathrm{d}P)_{\mathrm{II-I}} = -4{\cdot}4$ K kbar^{-1} and $(\mathrm{d}T/\mathrm{d}P)_{\mathrm{III-I}} = +17$ K kbar^{-1} at the triple point. The latent heat signals were about equal; using the values of ΔV measured by Jayaraman *et al.* we found them to be $\Delta H_{\mathrm{II-I}} = 0{\cdot}19$ cal g^{-1} and $\Delta H_{\mathrm{III-I}} = 0{\cdot}24$ cal g^{-1}, respectively, leaving $\Delta H_{\mathrm{II-III}} =$ 0·05 ± 0·05 cal g^{-1}. The fact that no latent heat signal was observed for the II–III transition indicates that $\Delta H_{\mathrm{II-III}} \lesssim 0{\cdot}02$ cal g^{-1}, and the slope of the II–III phase line is steeper than 240 K kbar^{-1}, but the sign of the slope is not determined. Bridgman's (1935) volume measurement between phases I and II appear unreliable.

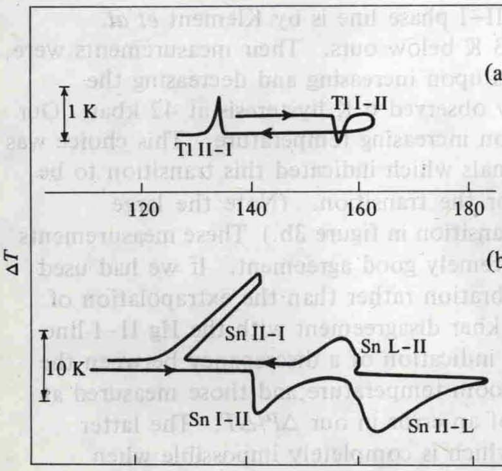

Figure 9. (a) DTA signals for the Tl III–I transition on increasing and decreasing temperature. (b) DTA signals for the Sn II–I melting transitions.

The phase diagram for tin is in excellent agreement with the work of Millet (1968), but the pressures reported by Kennedy and Newton (1963) are 2·5 kbar high even at the triple point where our pressure should be very accurate. The triple point values are given in table 2. Our measured slopes at the triple point are $(\mathrm{d}T/\mathrm{d}P)_{\mathrm{I-II}} = -2{\cdot}0$ K kbar^{-1}, $(\mathrm{d}T/\mathrm{d}P)_{\mathrm{I-L}} = +2{\cdot}0$ K kbar^{-1}, and $(\mathrm{d}T/\mathrm{d}P)_{\mathrm{II-L}} = +6{\cdot}1$ K kbar^{-1}. Assuming the ratio of the compressibility to the thermal expansion to be independent of temperature and pressure, we can calculate the volume below the triple point in phase I using compression measurements to 30 kbar of Barnett *et al.* (1966), and from Barnett *et al.* (1963) we find the volume in phase II giving $\Delta V_{\mathrm{I-II}} = -0{\cdot}0035$ cm^3 g^{-1} and $\Delta H_{\mathrm{I-II}} = 24$ cal g^{-1}. Taking the relative areas under the latent-heat peaks we find $\Delta H_{\mathrm{I-L}} = 50$ cal g^{-1} and $\Delta H_{\mathrm{II-L}} = 27$ cal g^{-1} with $\Delta V_{\mathrm{I-L}} = +0{\cdot}007$ cm^3 g^{-1} and $\Delta V_{\mathrm{II-L}} = 0{\cdot}011$ cm^3 g^{-1}. The Sn I–II solid–solid transition is very sharp and as shown in figure 9b it takes place at the equilibrium value. The Sn II–I phase change shows supercooling, but once the transition begins the temperature rises instantaneously to the equilibrium value. This solid–solid transition should be ideal for pressure calibration. It is probably a displacive transition as suggested by Musgrave (1963) and Barnett *et al.* (1963).

The solid–solid phase changes in bismuth all showed varying amounts of hysteresis. The triple points, reported in table 1, are estimates of the equilibrium transition points judged from the shape of the DTA signals on increasing and decreasing temperatures. The hysteresis is shown in figure 6 for some of the phase lines.

The method of measuring phase changes in a liquid hydrostatic medium is very easy and gives extremely reproducible results, and, once the problem of calibration has been better refined, it will be the most accurate method of measuring phase diagrams yet used. This experimental technique allowed us to obtain all triple points in the pressure range in the same experimental cell.

The pressure increase with temperature reported here is only meaningful for a high-pressure cell of the same geometry and materials as we used. This is clearly evidenced by the much smaller value found by Mitra *et al.* (1967) in a solid pressure cell with a much smaller fraction of the volume of the cell comprising the furnace. We also have evidence that at very low pressures, before the gaskets are well formed, the pressure increase is smaller than the value we report here. In fact, heating at very low loads will often allow the sample to 'blow out'. This work might be made more universally useful by calibrating the resistance of a Manganin wire against the pressure and temperature as determined by these phase diagrams. The stability of a Manganin gauge at these temperatures, however, may be questionable.

Table 2. Triple points in the phase diagrams of tin and thallium (°C/kbar).

Investigator	Sn I–II–L	Tl I–II–III
Dudley and Hall (1960)	318/31	
Kennedy and Newton (1963)	304/33	
Jayaraman *et al.* (1963)		115/38·5
Millet (1968)	308/30·1	
This work	307/29·5	106/37·3

Acknowledgements. We gratefully acknowledge helpful discussions with W. E. Evenson during this research. This work was supported in part by the National Science Foundation.

References

Akella, J., Ganguly, J., Grover, R., Kennedy, G. C., 1973, *J. Phys. Chem. Solids,* **34**, 631-636.

Barnett, J. D., Bean, V. E., Hall, H. T., 1966, *J. Appl. Phys.*, **37**, 875-877.

Barnett, J. D., Bennion, R. B., Hall, H. T., 1963, *Science,* **141**, 1041-1042.

Bogdanov, V. S., Levin, Yu. L., Sekoyan, S. S., Shimn, Yu. I., 1971, in *Accurate Characterization of the High Pressure Environment,* Ed. E. C. Lloyd, N.B.S. Special Publication 326 (US National Bureau of Standards, Washington, DC), pp.297-302.

Bridgman, P. W., 1935, *Phys. Rev.*, **48**, 893-906.

Butuzov, V. P., Ponyatovskii, E. G., 1956, *Sov. Phys. - Crystallogr.*, **1**, 453-455.

Candland, C. T., Decker, D. L., Vanfleet, H. B., 1972, *Phys. Rev.*, **B5**, 2085-2094.

Decker, D. L., 1965, *J. Appl. Phys.*, **36**, 157-161.

Decker, D. L., 1971, *J. Appl. Phys.*, **42**, 3239-3244.

Decker, D. L., Bassett, W. A., Merrill, L., Hall, H. T., Barnett, J. D., 1972, *J. Phys. Chem. Ref. Data,* **1**, 773-835.

Decker, D. L., Vanfleet, H. B., 1965, *Phys. Rev.*, **A138**, 129-133.

Dudley, J. D., Hall, H, T., 1960, *Phys. Rev.*, **118**, 1211-1216.

Getting, I. C., Kennedy, G. C., 1970, *J. Appl. Phys.*, **41**, 4552-4562.

Hanneman, R. E., Strong, H. M., Bundy, F. P., 1971, in *Accurate Characterization of the High Pressure Environment,* Ed. E. C. Lloyd, N.B.S. Special Publication 326 (US National Bureau of Standards, Washington, DC), pp.53-62.

Haygarth, J. C., Luedmann, H. D., Getting, I. C., Kennedy, G. C., 1969, *J. Phys. Chem. Solids,* **30**, 1417-1424.

Jayaraman, A., Klement, W., Newton, R. C., Kennedy, G. C., 1963, *J. Phys. Chem. Solids,* **24**, 7-18.

Kennedy, G. C., Newton, R. C., 1963, in *Solids under Pressure,* Eds W. Paul, D. Warschauer (McGraw-Hill, New York). pp.163-178.

Klement, W., Jayaraman, A., Kennedy, G. C., 1963a, *Phys. Rev.*, **131**, 1-6.

Klement, W., Jayaraman, A., Kennedy, G. C., 1963b, *Phys. Rev.*, **131**, 632-637.

Millet, L. E., 1968, "Experimental melting curves of cadmium, indium, lead, tin, and zinc and Mössbauer measurements in iron to 90 kilobars", unpublished dissertation, Brigham Young University, Provo, Utah.

Millet, L. E., Decker, D. L., 1969, *Phys. Letters,* **29A**, 7-8.

Mitra, N. R., Decker, D. L., Vanfleet, H. B., 1967, *Phys. Rev.*, **161**, 613-617.

Musgrave, M. J. P., 1963, *J. Phys. Chem. Solids,* **24**, 557-558.

Ponyatovskii, E. G., 1960, *Sov. Phys. - Crystallogr.*, **5**, 147-149.

Tikhomirova, N. A., Tonkov, E. Yu., Stishov, S. M., 1966, *JETP Letters,* **3**, 60-62.

Wang, C., 1967, *Rev. Sci. Instr.*, **38**, 24-26.

Young, R. K., 1969, "Equations of state for lithium fluoride and sodium metal to very high pressures and high temperatures", unpublished dissertation, Brigham Young University, Provo, Utah.